AMERICAN SOCIETY FOR MICROBIOLOGY | Applied and Environmental Microbiology®

FOOD MICROBIOLOGY

Biofilm Formation by *Listeria monocytogenes* 15G01, a Persistent Isolate from a Seafood-Processing Plant, Is Influenced by Inactivation of Multiple Genes Belonging to Different Functional Groups

Jessika Nowak,[a,b] Sandra B. Visnovsky,[c] Andrew R. Pitman,[e] Cristina D. Cruz,[a,d] Jon Palmer,[b] Graham C. Fletcher,[a] Steve Flint[b]

[a]The New Zealand Institute for Plant and Food Research Limited, Auckland, New Zealand
[b]Institute of Food, Nutrition and Human Health, Massey University, Palmerston North, New Zealand
[c]The New Zealand Institute for Plant and Food Research Limited, Lincoln, New Zealand
[d]Drug Research Program, Division of Pharmaceutical Biosciences, Faculty of Pharmacy, University of Helsinki, Helsinki, Finland
[e]The Foundation for Arable Research, Christchurch, New Zealand

ABSTRACT *Listeria monocytogenes* is a ubiquitous foodborne pathogen that results in a high rate of mortality in sensitive and immunocompromised people. Contamination of food with *L. monocytogenes* is thought to occur during food processing, most often as a result of the pathogen producing a biofilm that persists in the environment and acting as the source for subsequent dispersal of cells onto food. A survey of seafood-processing plants in New Zealand identified the persistent strain 15G01, which has a high capacity to form biofilms. In this study, a transposon library of *L. monocytogenes* 15G01 was screened for mutants with altered biofilm formation, assessed by a crystal violet assay, to identify genes involved in biofilm formation. This screen identified 36 transposants that showed a significant change in biofilm formation compared to the wild type. The insertion sites were in 27 genes, 20 of which led to decreased biofilm formation and seven to an increase. Two insertions were in intergenic regions. Annotation of the genes suggested that they are involved in diverse cellular processes, including stress response, autolysis, transporter systems, and cell wall/membrane synthesis. Analysis of the biofilms produced by the transposants using scanning electron microscopy and fluorescence microscopy showed notable differences in the structure of the biofilms compared to the wild type. In particular, inactivation of *uvrB* and *mltD* produced coccoid-shaped cells and elongated cells in long chains, respectively, and the *mgtB* mutant produced a unique biofilm with a sandwich structure which was reversed to the wild-type level upon magnesium addition. The *mltD* transposant was successfully complemented with the wild-type gene, whereas the phenotypes were not or only partially restored for the remaining mutants.

IMPORTANCE The major source of contamination of food with *Listeria monocytogenes* is thought to be due to biofilm formation and/or persistence in food-processing plants. By establishing as a biofilm, *L. monocytogenes* cells become harder to eradicate due to their increased resistance to environmental threats. Understanding the genes involved in biofilm formation and their influence on biofilm structure will help identify new ways to eliminate harmful biofilms in food processing environments. To date, multiple genes have been identified as being involved in biofilm formation by *L. monocytogenes*; however, the exact mechanism remains unclear. This study identified four genes associated with biofilm formation by a persistent strain. Extensive microscopic analysis illustrated the effect of the disruption of *mgtB*, *clsA*, *uvrB*, and *mltD* and the influence of magnesium on the biofilm structure. The results strongly suggest an involvement in biofilm formation for the four genes and provide a basis

Citation Nowak J, Visnovsky SB, Pitman AR, Cruz CD, Palmer J, Fletcher GC, Flint S. 2021. Biofilm formation by *Listeria monocytogenes* 15G01, a persistent isolate from a seafood-processing plant, is influenced by inactivation of multiple genes belonging to different functional groups. Appl Environ Microbiol 87:e02349-20. https://doi.org/10.1128/AEM.02349-20.

Editor Danilo Ercolini, University of Naples Federico II

Address correspondence to Sandra B. Visnovsky, sandra.visnovsky@plantandfood.co.nz.

Received 23 September 2020
Accepted 25 February 2021
Accepted manuscript posted online 19 March 2021
Published 27 April 2021

for further studies to analyze gene regulation to assess the specific role of these biofilm-associated genes.

KEYWORDS food safety, *Listeria monocytogenes*, biofilms, mutagenesis

The foodborne pathogen *Listeria monocytogenes* is a serious health threat to immunocompromised people, the elderly, pregnant women, and unborn and newborn babies (1), with a high mortality rate (up to 30%) in those groups (2). *L. monocytogenes* is ubiquitous in the environment, with contamination of food usually occurring during processing rather than being present in raw food (3, 4). The breadth of foods contaminated with *L. monocytogenes* is extensive and includes ready-to-eat meat and seafood, as well as vegetables and fruit (5).

L. monocytogenes is motile across a broad range of temperatures and has the capacity to adapt quickly to environmental changes to secure its survival. It can grow over a broad temperature range and survive freezing temperatures (6). *L. monocytogenes* can tolerate some degree of low pH but is not as acid tolerant as some other foodborne pathogenic bacteria, such as *Escherichia coli* O157:H7. It is also capable of surviving in high salt concentrations up to 11.5% (6). All of these attributes contribute to the adaptability of this pathogen and impede its control when encountered in food-processing environments.

Surface attachment and biofilm formation are important to the environmental persistence of *L. monocytogenes* (7). A biofilm is a community of cells that exists in a sessile lifestyle rather than a planktonic one in order to use resources more efficiently and to resist environmental threats. Cells in a biofilm are attached to each other and to a surface. They are held together by an extracellular polymeric matrix that consists of DNA, proteins, lipopolysaccharides, and other substances that contribute to its stability and act as a protective barrier. For *L. monocytogenes*, the capacity to form biofilms in so-called "harborage" sites enables the pathogen to establish itself and to act as a source for subsequent dispersal of single cells. Management of *L. monocytogenes* is further impaired because biofilm cells are more resistant to cleaning agents and sanitizers (8), as well as antibiotics (9). As a result, *L. monocytogenes* is able to contaminate both surfaces and food products.

Transposon mutagenesis has proven to be a successful tool for identification of genes involved in biofilm formation by *L. monocytogenes* (10, 11). As a result, to date, four research groups have successfully identified genes involved in biofilm formation by *L. monocytogenes* using the Himar1-based transposition system (12–15). The majority of the identified genes were associated with biosynthesis or motility. This transposition system has also been used to identify the genetic factors underlying other phenotypic changes, such as desiccation survival or nisin sensitivity (16, 17).

A survey of seafood-processing plants in New Zealand identified four persistent strains (persisted in factories for at least 6 months), classified by their unique pulsotypes (18). One of these pulsotypes (type 5132), represented by *L. monocytogenes* 15G01, was shown to have a high capacity to form biofilms in *in vitro* assays (18–20). Further genomic studies revealed that *L. monocytogenes* 15G01 (lineage II genome) belongs to the sequence type ST-321, determined using MLST, and is lacking the φtRNA-Ser prophage (20). This isolate exhibited low invasion in mammalian cell cultures (20), which is linked to truncation of the primary virulence factor internalin A (InlA) (21). Since the capacity to form biofilms is believed to be a major contributing factor in persistence of *L. monocytogenes* and subsequent contamination of food in food-processing premises, a library of mutants of *L. monocytogenes* 15G01, previously generated using the Himar1 mariner-based transposition system (22), was screened for mutants with altered biofilm formation using the crystal violet assay. This study aimed to reveal additional genes in *L. monocytogenes* 15G01 that are associated with biofilm formation and to further characterize the role of these genes through visualization of the structure by using scanning electron microscopy (SEM) and fluorescence microscopy to visualize the structure of the altered biofilms.

TABLE 1 Biofilm-related genes identified in *L. monocytogenes* 15G01 through transposon insertions based on DNA homologies with the *L. monocytogenes* EGD genome database (accession number HG421741)[a]

Function group and putative gene function	Transposon insertion site	Mean biofilm mass (%) relative to WT ± SD	No. of hits	Coordinate(s) for insertion in *L. monocytogenes* EGD	Orientation of transposon insertion	Mutant strain[b]
Biosynthesis						
Adenylosuccinate synthase	*LMON_0057* (*purA*)	135.7 ± 5.12	1	59174	3′–5′	24A10
Dihydroxyacetone kinase family protein	*LMON_1882*	173.03 ± 7.82	1	1888930	3′–5′	35H9
Acetyltransferase, GNAT family	*LMON_2362*	27.32 ± 6.92	1	2377834	5′–3′	31E7
Glycosyl hydrolase, family 31	*LMON_2457*	19.90 ± 4.93	1	–[d]	3′–5′	32E5
Cell wall/membrane						
Sortase A, LPXTG-specific SrtA	*LMON_0935*	7.49 ± 0.59	1	948604	3′–5′	31C7
Glycosyltransferase	*LMON_0939*	18.74 ± 3.36	1	–	5′–3′	35C1
Putative peptidoglycan-bound protein (LPXTG motif) Lmo1666 homologue	*LMON_1733*	29.70 ± 5.66	3	1723653, 1721718, 1721318	5′–3′, 3′–5′, 3′–5′	24H3, 25D2, 64B3
Cardiolipin synthetase ClsA	*LMON_2515*	163.02 ± 15.27	2	2538121, 2538525	3′–5′, 5′–3′	30A9, 34F11
Glycosyltransferase LafA	*LMON_2570*	16.10 ± 2.43	2	2591134, 2590370	3′–5′, 3′–5′	28G11, 32A9
Translation and transcription						
GTP-binding protein HflX	*LMON_1358*	16.06 ± 6.92	1	–	3′–5′	43C9
SSU ribosomal protein S1p	*LMON_2007* (*rpsA*)	140.68 ± 10.74	1	2012734	3′–5′	28A2
Transporter systems						
Manganese ABC transporter, ATP-binding protein SitB	*LMON_1917*	133.83 ± 7.38	1	1925244	3′–5′	47H11
Bacitracin export ATP-binding protein BceA	*LMON_2188*	138.01 ± 1.19	1	2194403	3′–5′	31G1
ABC transporter, permease protein EscB	*LMON_2290*	142.51 ± 7.66	2	2305608, 2305511	3′–5′, 3′–5′	32E2, 47H10
Phosphate ABC transporter, periplasmic phosphate-binding protein PstS	*LMON_2511*	30.81 ± 0.50	1	2532962	3′–5′	36A2
PTS system, IIA component	*LMON_2675*	32.69 ± 3.94	1	2692293	3′–5′	26C10
Mg^{2+} transport ATPase, P-type	*LMON_2712*	7.16 ± 1.47	2	2731046, 2731895	3′–5′, 3′–5′	30H2, 44D3
ABC transporter, ATP-binding protein	*LMON_2792*	6.93 ± 0.27	1	2816670	3′–5′	28D10
Motility						
Flagellin protein FlaA	*LMON_0695* (*flaA*)	23.74 ± 5.93	1	–	3′–5′	41H7
Autolysis						
Membrane-bound lytic murein transglycosylase D precursor MltD	*LMON_2714*	2.11 ± 0.35	1	2734305	5′–3′	39G5
DNA repair and stress response						
Glutamate decarboxylase	*LMON_2376*	6.81 ± 0.93	1	2393310	3′–5′	35F3
Excinuclease ABC subunit B UvrB	*LMON_2501* (*uvrB*)	18.33 ± 2.58	2	2525427, 2525564	3′–5′, 3′–5′	33E11, 42G3
Unknown						
FIG00774663: hypothetical protein	*LMON_1212*	21.32 ± 0.69	1	–	5′–3′	36B9
FIG00774466: hypothetical protein	*LMON_2144*	28.89 ± 3.37	1	2153693	5′–3′	26H1
COG1801: uncharacterized conserved protein	*LMON_2417*	15.37 ± 0.51	1	–	3′–5′	40C12
Hypothetical protein (mutant strain 44F5)	NC[c]	10.70 ± 5.02	1	–	3′–5′	44F5
Hypothetical protein (mutant strain 41A8)	NC	21.88 ± 7.19	1	–	3′–5′	41A8
Intergenic[e]		18.27 ± 1.96	1	2450096	3′–5′	67C5

(Continued on next page)

TABLE 1 (Continued)

Function group and putative gene function	Transposon insertion site	Mean biofilm mass (%) relative to WT ± SD	No. of hits	Coordinate(s) for insertion in *L. monocytogenes* EGD	Orientation of transposon insertion	Mutant strain[b]
Methionine ABC transporter ATP-binding protein and hypothetical protein	*LMON_2430* and *LMON_2431*					
Dihydroxyacetone kinase family protein and putative alkaline-shock protein	*LMON_1882* and *LMON_1883*	173.44 ± 15.52	1	1889436	3′–5′	33F8

[a]Homologies were identified by Megablast and Geneious 7 software using default settings. The biofilm mass produced by the mutants (CV assay) was calculated relative to the biofilm formation by the wild type in two independent experiments with eight replicates. Putative gene functions are based on information from http://www.genome.jp/.
[b]Internal numbering of the transposon library.
[c]NC, no counterpart in *L. monocytogenes* EGD but present in the parental strain.
[d]–, the exact insertion site could not be determined.
[e]Defined by the two genes at each boundary of the intergenic space. 67C5 is 217 bp downstream of LMON_2430 and 100 bp upstream of LMON_2431, while 33F8 insertion is 7 bp downstream of LMON_1882 and 373 bp upstream of LMON _1883.

RESULTS

An *in vitro* biofilm assay identified multiple mutants that have either more or less biofilm formation than does the wild type. A set of 4,500 mutants of a transposant library of approximately 6,500 mutants of *L. monocytogenes* 15G01, created with the mariner transposition system, was screened at 30°C in modified Welshimer's broth (MWB) for mutants with altered biofilm formation using the 1% aqueous crystal violet (CV) assay (a set of 2,000 mutants has been analyzed previously (20). These conditions were used since they had been previously shown to induce biofilm formation by *L. monocytogenes* 15G01 (19). In total, 36 mutants were found with greater (10 mutants) or lower (26 mutants) biofilm formation ability under these conditions compared to the wild type (Table 1), with the average optical density at 595 nm (OD_{595}) of the mutants being at least two standard deviations (SD) below or above the average OD_{595} value (1.197) of the wild-type strain, *L. monocytogenes* 15G01. The growth of the mutants was compared to the growth of the wild-type strain in MWB during the screen to confirm that the altered biofilm formation observed was not due to differences in the ability of the mutants to grow in this media, and only mutants showing equal or higher OD_{595} than the wild type after 48 h were included.

Characterization of the transposon insertion sites in mutants with altered biofilm formation identified 27 loci potentially involved in this process. Nested semiarbitrary PCR enabled the amplification of the genome sequences flanking the transposons in the 36 mutants. DNA sequencing of the flanking regions and subsequent BLASTN and Megablast comparisons of the sequences with the genome of reference strain *L. monocytogenes* EGD permitted the locations and directions of the insertions in 15G01 to be estimated for all mutants, with identification of the exact insertion sites for 28 mutants (Table 1). Transposon insertions seemed to predominantly occur in the second half of the genome raising doubts as to the random nature of transposition (see Fig. S3a in the supplemental material). In the 36 mutants examined, 27 genes were disrupted by a transposon insertion, with six loci disrupted in two independent mutants and one disrupted in three independent mutants (Table 1). Two mutants had an insertion of the transposon in an intergenic region (Table 1), and a further two mutants had insertions in genes that were not present in the reference genome of *L. monocytogenes* EGD but in the parental strain *L. monocytogenes* 15G01.

Functional analysis of the disrupted genes identified multiple functional groups involved in biofilm formation by *L. monocytogenes* 15G01. Comparison of the disrupted genes in each of the mutants affected in biofilm formation with homologous genes in *L. monocytogenes* EGD and other *L. monocytogenes* strains in the GenBank database divided them into seven diverse functional groups (Table 1). Of particular note, five genes annotated as being involved in cell wall/membrane synthesis

TABLE 2 *L. monocytogenes* strains and plasmids used in this study

Strain or plasmid	Description	Mutation	Source or reference
Strains			
15G01	Wild-type serotype 1/2a; Em^s Kan^s		18
34F11	15G01 with transposon inserted in the *clsA* gene (*LMON_2515*); Em^r Kan^s	15G01 *clsA*::himar1	This study
33E11	15G01 with transposon inserted in the *uvrB* gene (*LMON_2501*); Em^r Kan^s	15G01 *uvrB*::himar1	This study
33E11-C	33E11 containing the pIMK-uvrB plasmid; Em^r Kan^r	15G01 *uvrB*::himar1/pIMK*uvrB*	This study
33E11-EV	33E11 containing the pIMK plasmid; Em^r Kan^r	15G01 *uvrB*::himar1/pIMK	This study
39G5	15G01 with transposon inserted in the *mltD* gene (*LMON_2714*); Em^r Kan^s	15G01 *mltD*::himar1	This study
39G5-C	39G5 containing the pIMK-mltD plasmid; Em^r Kan^r	15G01 *mltD*::himar1/pIMK*mltD*	This study
39G5-EV	39G5 containing the pIMK plasmid; Em^r Kan^r	15G01 *mltD*::himar1/pIMK	This study
44D3	15G01 with transposon inserted in the *mgtB* gene (*LMON_2712*); Em^r Kan^s	15G01 *mgtB*::himar1	This study
41H7	15G01 with transposon inserted in the *flaA* gene (*LMON_0695*); Em^r Kan^s	15G01 *flaA*::himar1	This study
Plasmids			
pIMK	Site-specific listerial integrative vector, 5.1 kb; Kan^r		80
pIMK-uvrB	Site-specific plasmid carrying the *LMON_2501* gene; Kan^r		This study
pIMK-mltD	Site-specific plasmid carrying the *LMON_2714* gene; Kan^r		This study

or integrity were identified, including genes encoding a putative peptidoglycan-bound protein disrupted in three mutants that had low biofilm formation, cardiolipin synthetase (designated *clsA*), disrupted in two mutants with greater biofilm formation and the glycosyltransferase LafA in two mutants with low biofilm formation.

Genes involved in transport systems, stress response, autolysis, and motility also influenced biofilm formation, including a gene predicted to encode a P-type Mg^{2+} transport ATPase (designated *mgtB*) and a gene annotated as encoding the ABC transporter permease protein EscB, which were both disrupted in two mutants. Disruption of the P-type Mg^{2+} transport ATPase resulted in decreased biofilm formation, while the insertion of the transposon into *escB* resulted in increased biofilm formation.

Complementation of selected genes confirms a role for *mltD* in biofilm formation by *L. monocytogenes* 15G01. Four mutants (33E11, 34F11, 39G5, and 44D3) were examined further to confirm the role of the disrupted genes in biofilm formation by *L. monocytogenes* 15G01 (Table 2). The first, the *clsA* mutant (34F11), was selected because this gene had been disrupted in multiple mutants with increased biofilm formation and because the *clsA* gene was known to be involved in biofilm formation by other bacterial species (23–25). The *uvrB* mutant (33E11) was selected since multiple mutants with a transposon insertion in the gene coding for the excision nuclease ABC subunit B were identified in the screen and *uvrB* is part of an operon with *uvrA*, which, when disrupted in *L. monocytogenes* in a previous study, resulted in increased biofilm formation at 15°C (15). The *mltD* mutant (39G5) was studied because it was predicted to affect autolysis, which has been implicated in changes in biofilm formation by *L. monocytogenes* (26, 27) and other bacteria (28), while the *mgtB* mutant (44D3) was included because it has also been disrupted in multiple mutants and has not been associated with biofilm formation by *L. monocytogenes* before.

Growth curves of the selected 36 mutants in MWB at 30°C were then produced by manual measurements to further examine growth behavior (see Table S1 and Fig. S1 in the supplemental material) in the presence of erythromycin (the transposon contains an erythromycin resistance gene). In addition, growth studies with an automated plate reader were carried out for the four selected mutants without selective antibiotics to further rule out the possibility that the changes in biofilm formation were due to impaired growth (see Fig. S2). The two mutants 39G5 and 44D3 formed cell aggregates during growth which is reflected by the high OD_{600} values; however, the growth pattern was not affected. 39G5 had an extended exponential phase compared to the other strains, but all five examined strains were in stationary phase at 48 h, the time point at which biofilm formation was measured.

Complementation studies were subsequently carried out on the four mutants. In these studies, introduction of the pIMK vector containing the wild-type *mltD* gene into

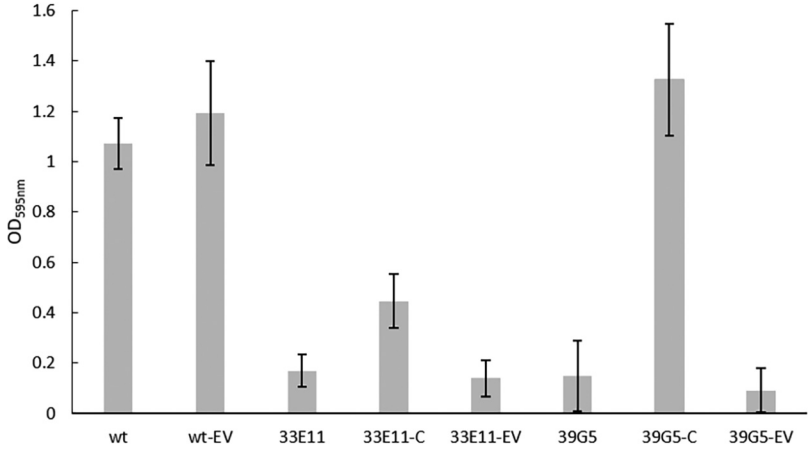

FIG 1 Comparison of biofilm formation by *L. monocytogenes* 15G01 (wt), the *uvrB* and *mltD* mutants (33E11 and 39G5), and mutants containing a wild-type copy of the corresponding gene (complemented strains [-C]) or the empty vector pIMK (-EV). Error bars represent the SD for three independent experiments ($n = 6$). Biofilm formation was determined by measuring the OD_{595} as part of the CV assay.

the *mltD* mutant resulted in the restoration of biofilm formation to levels produced by the wild type (Fig. 1). Conjugation of the empty vector into this mutant had no obvious effect on biofilm formation (Fig. 1). These data confirmed that the change in biofilm formation by the *mltD* (a homologue of the peptidoglycan hydrolase *murA*) mutant was a result of inactivation of the gene. Thus, *mltD* is required for biofilm formation by *L. monocytogenes* 15G01.

In contrast to the successful complementation of the *mltD* mutant (39G5), introduction of the pIMK vector containing the wild-type *uvrB* gene into the *uvrB* mutant only partially restored (41.7%) the wild-type phenotype (Fig. 1), while attempts to complement the *mgtB* and *clsA* mutants (44D3 and 34F11) using a similar process failed to restore the wild-type phenotype altogether (data not shown).

Microscopy confirmed that the *mltD* mutant (39G5) experiences a dramatic loss in both viable and nonviable cells. All of the selected mutants were included in microscopic analysis to assess changes in phenotype despite the failure to complement a number of the mutations. Fluorescence microscopy showed that, after 48 h of incubation of the mutants on polystyrene surfaces in MWB at 30°C, all appeared to show some differences in the structure of their biofilms compared to the wild type (Fig. 2). The biofilm of the *mltD* mutant (39G5) (Fig. 2d) consisted of a few (mainly individual) cells, which seemed to be elongated and in chains. The lack of visible cells (whether alive or dead) was consistent with the low biofilm formation observed in the initial screen. The biofilm produced by the *mgtB* mutant (44D3) also contained few live cells, although it did appear to have a cloudy structure under fluorescence (Fig. 2e). Consistent with this, there appeared to be greater numbers of dead cells associated with the biofilm produced by the *mgtB* mutant. The *uvrB* mutant (33E11) was a low biofilm former and exhibited only sparse biofilm formation after 48 h (Fig. 2c), which was consistent with the approximately 80% reduction in biofilm formation observed in *in vitro* assays. The *clsA* mutant (34F11) showed a biofilm with a high number of living cells but also showed a larger amount of dead, red-stained cells (Fig. 2b).

SEM was used to analyze further the structure of the biofilms produced by the mutants after growth of the bacteria on stainless-steel (SS) coupons coated with mussel juice for 7 days at 30°C. An SS coupon coated with mussel juice was used as a control, and organic debris was clearly visible (Fig. 3k and l). Bacterial cells attached and formed biofilms on the coupons preferably where organic debris of the mussel juice was present (Fig. 3i and j).

SEM images of 39G5 confirmed the long-chain phenotype with some elongated cells (Fig. 3g and h). Transposon mutant 33E11 was a low biofilm former and exhibited

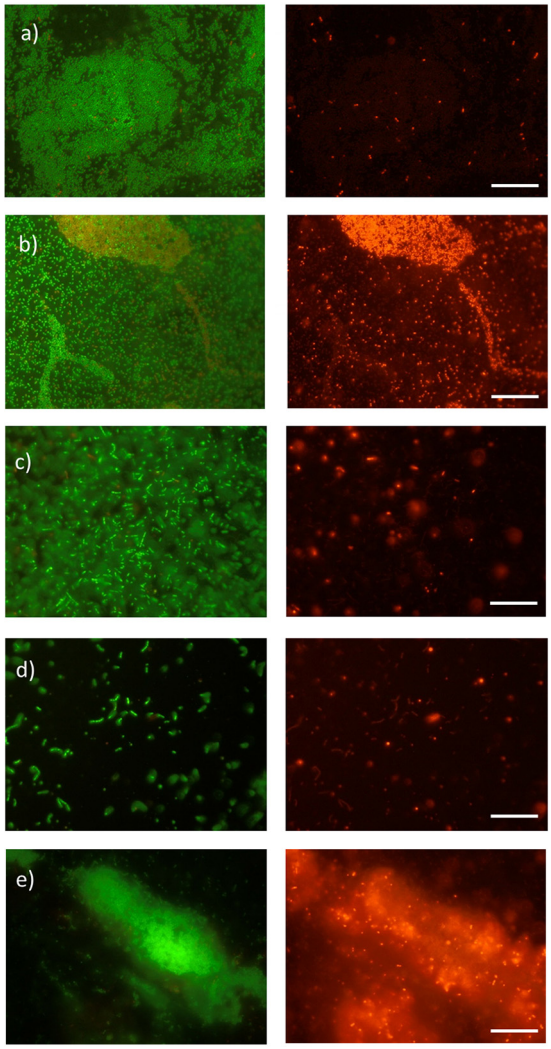

FIG 2 Images of the biofilms produced by *L. monocytogenes* 15G01 (wild type) (a) and selected transposon mutants with altered biofilm formation (34F11 [b], 33E11 [c], 39G5 [d], and 44D3 [e]) grown on polystyrene surfaces in MWB for 48 h at 30°C. The biofilms were stained with a Live/Dead *Bac*Light bacterial viability kit according to the manufacturer's instructions (Life Technologies, Thermo Fisher, New Zealand). Living cells were labeled with SYTO9 (green) and dead cells with propidium iodide (red). Scale bars, 20 μm. Mutants: 34F11, *clsA* mutant; 33E11, *uvrB* mutant; 39G5, *mltD* mutant; 44D3, *mgtB* mutant.

only sparse biofilm formation on SS coupons after 7 days, although extracellular matrix was present. 33E11 appeared to have a different cell morphology compared to the wild type, with coccoid-shaped rather than rod-shaped cells (Fig. 3e and f). Transposon mutant 34F11, identified as a high biofilm former in both the microtiter plate screening test and under the fluorescence microscope, also exhibited greater biofilm formation on the SS coupons compared to the wild type (Fig. 3c and d). In addition, 34F11 exhibited an extensive thread structured biofilm attached to organic mussel debris (Fig. 3d).

Confocal analysis reveals a unique sandwich structure for the biofilm of the *mgtB* mutant. The influence of magnesium on the biofilm structure was investigated using confocal analysis. COMSTAT was used to calculate the biomass, roughness, and maximum and average thickness of the biofilms (Table 3).

Isosurface images of the biofilms stained with SYTO 9 were generated with Imaris (Bitplane, Zurich, Switzerland). The wild-type control formed microcolonies on glass after 7 days of incubation in MWB at 30°C (Fig. 4g and h). In contrast to the CV assay (Fig. 4a and b), where magnesium addition did not alter biofilm amount significantly,

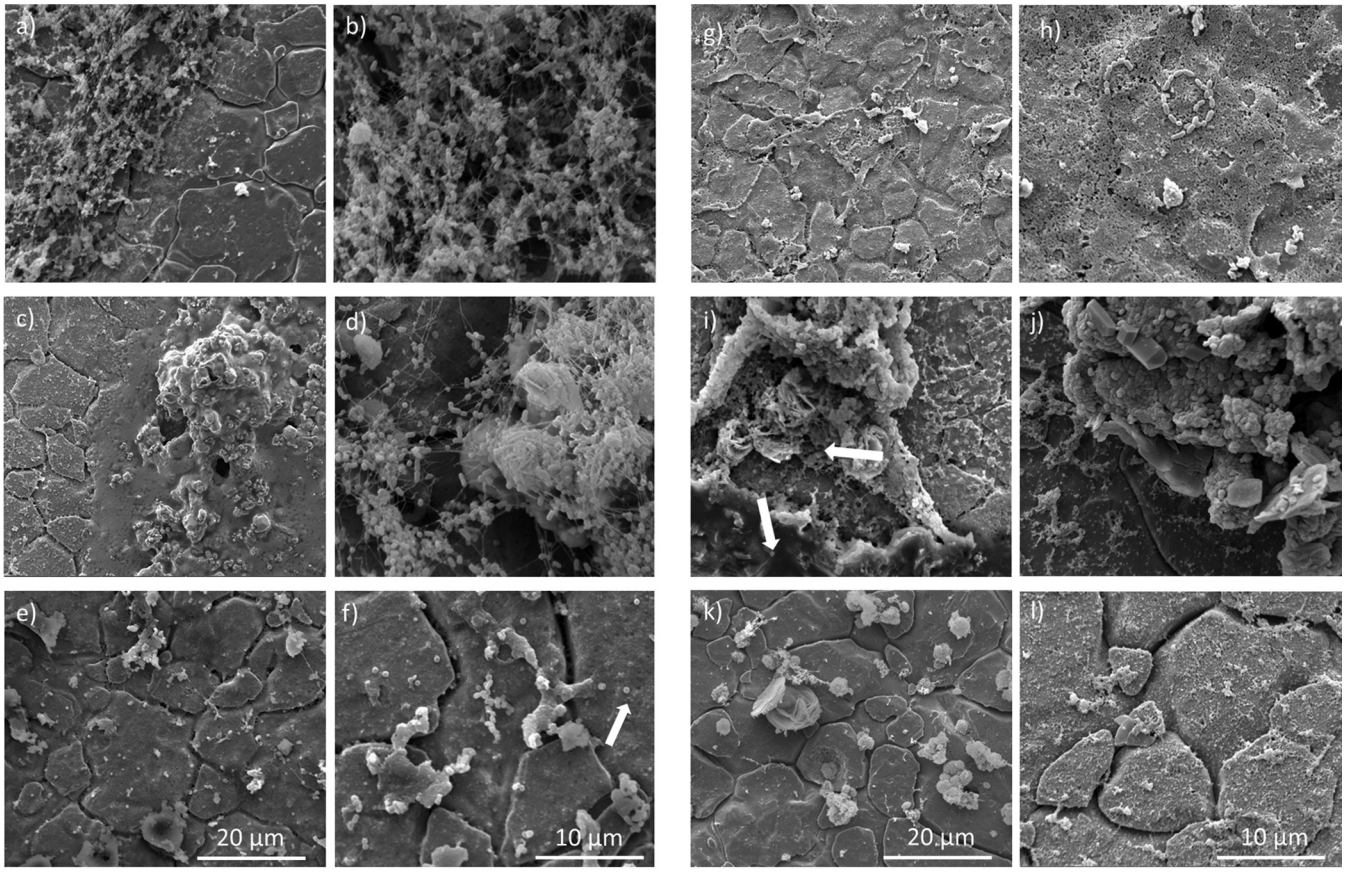

FIG 3 Images of the coupon coated with mussel juice (k and l) and the biofilms produced by *L. monocytogenes* 15G01 (wild type) (a and b) and selected transposon mutants with altered biofilm formation (34F11, *clsA* mutant [c and d]; 33E11, *uvrB* mutant [e and f]; 39G5, *mltD* mutant [g and h]; 44D3, *mgtB* mutant [i and j]) grown on stainless steel coupons coated with mussel juice for 7 days at 30°C. The images were obtained with a scanning electron microscope at 5,000× and 10,000× magnifications. The cracks are features of the stainless-steel surface. The white arrows point at coccoid-shaped bacteria (f) and two different types of biofilm (i).

biomass was reduced in the presence of 5 mM Mg^{2+} for the wild type when analyzed by confocal laser scanning microscopy (CLSM). However, the maximum thickness and the average thickness of the biomass remained the same when analyzed by CLSM. It is possible that magnesium led to increased production or stabilization of extracellular polymeric substance (which is not detected by CLSM) for the wild type. In addition, biofilms were formed on two different surfaces (polystyrene and glass), which could have also contributed to the observed differences.

Since the differences in biofilm mass in the presence of 5 mM Mg^{2+} were greatest when the *mltD* mutant 39G5 was incubated at 37°C (Fig. 4b), this temperature was

TABLE 3 Biomass, roughness coefficient, maximum thickness, and average thickness values for of biofilms formed by WT and mutants 39G5 (*mltD* mutant) and 44D3 (*mgtB* mutant) strains[a]

	Result (SD)					
Parameter	**WT**	**WT-Mg^{2+}**	**39G5**	**39G5-Mg^{2+}**	**44D3**	**44D3-Mg^{2+}**
Biomass ($\mu m^3/\mu m^2$)	1.145 (0.054)	0.497 (0.409)	1.813 (1.620)	0.191 (0.043)	0.841 (1.130)	1.626 (0.950)
Roughness coefficient (Ra*)	0.639 (0.074)	1.515 (0.256)	0.891 (0.750)	1.787 (0.009)	1.284 (0.874)	0.654 (0.455)
Maximum thickness (μm)	4.784 (1.452)	4.951 (0.317)	9.162 (3.767)	4.280 (0.00)	10.966 (6.764)	5.077 (0.262)
Avg thickness (entire area) (μm)	2.295 (0.776)	0.840 (0.561)	4.063 (2.399)	0.320 (0.089)	3.107 (4.807)	2.398 (1.340)
Avg thickness (biomass) (μm)	3.357 (1.377)	3.281 (0.533)	7.408 (2.243)	3.026 (0.913)	4.904 (4.283)	3.238 (1.082)

[a]The biomass, roughness coefficient, maximum thickness, and average thickness of biofilms formed by the wild type (WT) and the mutants 39G5 (*mltD* mutant) and 44D3 (*mgtB* mutant) in MWB and MWB with a final concentration of 5 mM Mg^{2+} after incubation at 30°C for 7 days were calculated using COMSTAT. Standard deviations were calculated from three analyzed images taken of each sample.

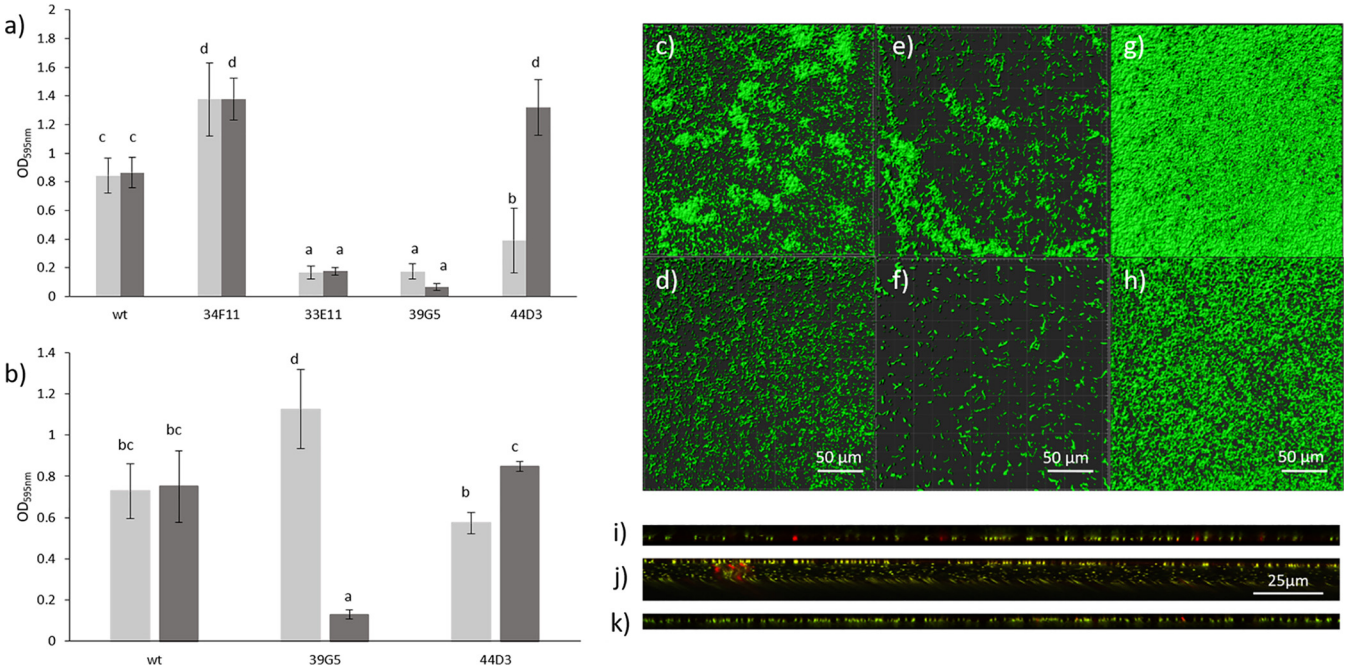

FIG 4 Biofilm formation by the wild type and selected mutants in MWB (light gray bars) and MWB with a Mg^{2+} concentration of 5 mM (dark gray bars) at 30°C (a) and 37°C (b) after 48 h of incubation measured with a CV assay. Error bars represent the SD of three independent experiments ($n = 6$). Letters in common indicate no significant difference. (c to h) Isosurface images of biofilms of wild-type (c), 39G5 (e), and 44D3 (g) strains formed on glass after 7 days of incubation in MWB (1.67 mM Mg^{2+}) and in MWB with a final Mg^{2+} concentration of 5 mM (wild type [d], 39G5 [f], and 44D3 [h]). Biofilms were grown at 30°C (wild type, 44D3) or 37°C (39G5) and stained with SYTO9. Orthogonal view of biofilms formed on a glass surface after 7 days at 30°C by the wild type in MWB (i), by the *mgt*B mutant (44D3) in MWB (j), and by the *mgtB* mutant (44D3) in the presence of 5 mM Mg^{2+} (k). Images were taken after removal of media and staining with a Live/Dead *Bac*Light kit with a confocal laser scanning microscope.

used for the CLSM analysis. The presence of magnesium led to a decrease in biofilm and attached cells for 39G5 after 7 days of incubation at 37°C (Fig. 4e and f). This was also observed with the CV assays after 48 h (Fig. 4a and b). The maximum thickness and average thickness were more than halved in the presence of 5 mM Mg^{2+} (46.71 and 40.84%, respectively, of the thicknesses without additional magnesium) (Table 3).

44D3 (*mgtB* mutant) produced more biofilm mass in the presence of 5 mM Mg^{2+} compared to 1.67 mM Mg^{2+} and less biomass than the wild type when grown in MWB (1.67 mM Mg^{2+}) (Table 3), a finding in line with the observations made with the CV assay (Fig. 4a). Calculations with COMSTAT revealed a double maximum thickness for the biofilm of 44D3 compared to biofilms formed by the wild type and 44D3 in the presence of 5 mM Mg^{2+} (Table 3). This suggests that Mg^{2+} restored the wild-type phenotype for the *mgtB* mutant (44D3) (Fig. 4g to k; Table 3). Mutant 44D3 produced a unique sandwich structure for the biofilm (Fig. 4j) with monolayers of bacterial cells at the top and bottom and extrapolymeric substance (EPS) or fluid in between. This structure has, to the best of our knowledge, not been reported for a biofilm before. In the presence of 5 mM Mg^{2+}, 44D3 produced a biofilm similar in structure to the wild type (Fig. 4i and k), further strengthening the hypothesis of restoration of the wild-type phenotype.

The *mltD* mutant (39G5) was defective in autolysis and motility, as well as in biofilm formation. Inactivation of *mltD* (a *murA* homologue) has previously been shown to result in loss of motility in *L. monocytogenes* (27). Consistent with these findings, the *mltD* mutant created in this study exhibited no motility (Fig. 5b), which was restored upon gene complementation (Fig. 5b). The Triton X-100-induced autolysis rate was reduced for the *mltD* mutant compared to the wild type (Fig. 5a), confirming the direct involvement in autolysis.

Furthermore, the *mltD* mutant, 39G5, produced less biofilm than the wild type at 30°C but more than the wild type at 37°C. At both temperatures, the presence of magnesium (5 mM) reduced biofilm production to a minimum when measured with the CV assay and by CLSM. Attachment studies revealed that the presence of magnesium did

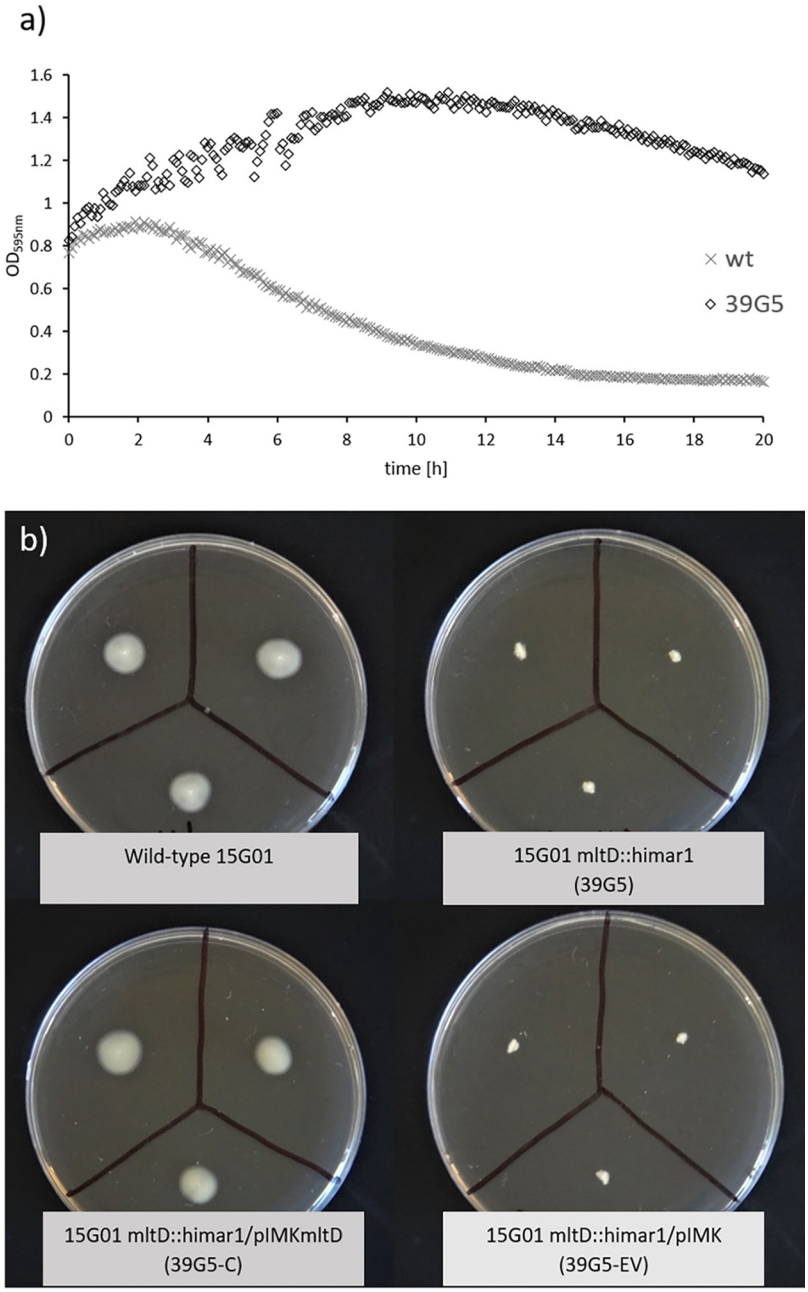

FIG 5 (a) Triton X-100-induced autolysis of *L. monocytogenes* 15G01 (wt) and the *mltD* mutant (39G5) determined by optical density measurement at 595 nm and (b) motility of *L. monocytogenes* 15G01 (top left), the *mltD* mutant (39G5 [top right]), and the *mltD* mutant containing a wild-type copy of the corresponding gene (39G5-C [bottom left]) or the empty vector pIMK (39G5-EV [bottom right]) after 24 h at 30°C.

not alter the attachment ability of 39G5, suggesting that magnesium influences the biofilm maturation process rather than surface characteristics or initial attachment (see Fig. S5 in the supplemental material).

Observations of both planktonic cells and biofilm cells in the present study using fluorescence microscopy (Fig. 2) and SEM (Fig. 3g and h) showed a high number of elongated cells in long chains for the *mltD* mutant.

The *mltD* mutant was found to produce increased cell aggregation, which interfered with optical density measurements for growth behavior. However, cell counts after 24 h

growth were similar to the wild-type levels (>9.0 $\log_{10}$ CFU/ml) (see Table S1 in the supplemental material).

DISCUSSION

We identified here 27 genes that are involved in *L. monocytogenes* 15G01 biofilm formation. Four other research groups have also used Himar1 transposon mutagenesis to identify genes involved in biofilm formation by *L. monocytogenes* (12–15). In each case, a large number of loci were reportedly associated with biofilm formation. Many of the loci were only identified in a single study, however, probably because different isolates and different assay conditions were used. For example, Piercey et al. (15) performed the assays at 15°C, while other groups used higher temperatures (32, 35, or 37°C). We opted to carry out our analysis at 30 and 37°C, even though food processing plants operate at a lower temperature. These temperatures were chosen for this high-throughput screen to identify potential biofilm associated genes in a timely manner since lower temperatures require longer incubation times due to a lower growth rate.

All studies, including this one, showed that a transposon insertion in *lafA* (gene ID *lmo2555* in *L. monocytogenes* EGDe), a gene encoding a glycosyltransferase required for membrane development, caused a reduction in biofilm formation (29). Other genes identified by us and other research groups included genes coding for sortase A, a peptidoglycan-linked protein (LPXTG), and the flagellum protein FlaA (13). The detection of common genes associated with changes in biofilm formation under such variable conditions suggests that they are critical to biofilm formation regardless of the environmental conditions the bacterium experiences.

This study revealed the probable involvement of *uvrB* in biofilm formation. Piercey et al. (15) identified *uvrA* (located in the same operon as *uvrB*), which was also associated with biofilm formation. Our research group, as well as Piercey et al. (15), used a serotype 1/2a strain isolated from a processing plant to generate the transposon library.

Ouyang et al. (14) and Alonso et al. (12) both generated a mutant library using *L. monocytogenes* 10403S, and Chang et al. (13) created a library of *L. monocytogenes* Scott A mutants. The *uvrAB* cluster was not identified as involved in biofilm formation in these other studies, suggesting either that the regulatory cascades controlling biofilm formation may be specific to certain environmental triggers or that they may be influenced by genetic variability between strains or serotypes.

Transporter systems are essential in living organisms. The transition from a planktonic to a sessile lifestyle requires changes in metabolism and energy generation as resources within biofilms become scarce (30). Thus, during the screening of the *L. monocytogenes* 15G01 mutants, it was not surprising to identify seven genes involved in these broad processes that influence biofilm formation.

One transporter system of particular interest is the P-type ATPase, which takes up Mg^{2+} upon ATP hydrolysis (MgtB). Previous studies have showed that magnesium deprivation triggers biofilm formation (31), and temperature-dependent expression (32) of *mgtB* is regulated by the PhoP/PhoQ two-component system in Gram-negative bacteria (33, 34). However, knowledge about the function of this P-type ATPase in Gram-positive bacteria, *L. monocytogenes* in particular, is limited. No data about the involvement of *mgtB* in biofilm formation are currently available. According to Nielsen et al. (35), *mgtB* (lmo2689) is regulated by the two-component system CesRK. CesR binding boxes were found upstream of this *mgtB* gene, which suggests direct control of *mgtB*. The *mgtB* gene is part of an operon including genes encoding cell division proteins (i.e., *ftsW*; see Fig. S3b) which are also regulated by CesR (35). CesRK is associated with virulence (36) and ethanol sensitivity and antibiotic sensitivity (37). The transposon insertion in the *mgtB* gene (44D3) resulted in the production of a low-biofilm phenotype in this study, suggesting the involvement of *mgtB* in biofilm formation by *L. monocytogenes*. The involvement of *mgtB* in biofilm formation has also been shown for *Cronobacter sakazakii* (38), wherein a disruption of *mgtB* led to a 77% reduction in biofilm mass. Other magnesium transporters (MgtE) have also been shown to be involved

in biofilm formation or potentially even in virulence (39). Of particular interest in this study was the observed sandwich structure of the biofilm formed by 44D3 with static monolayers at the top and bottom and movement in the fluid in between (Fig. 4). Similarly, Guilbaud et al. (40) also observed movement in the fluid in hollow structures of the biofilm when analyzing it by CLSM. Magnesium has been shown to influence biofilm formation by other bacterial species (31, 41), where high magnesium concentrations (50 mM and higher) led to reduced biofilm formation by *Bacillus subtilis* and *Bacillus cereus* (41) without affecting the growth. However, lower concentrations of 5 and 10 mM led to an increase in biofilm formation by *B. subtilis* in the same study. Other studies showed that Mg^{2+} presence led to increased attachment of *P. fluorescens* cells to glass (42), but, on the other hand, Mg^{2+} limitation resulted in increased biofilm formation by *Pseudomonas aeruginosa* through repression of the *retS* gene which is responsible for EPS biosynthesis (31). Although the findings are contradictory, it is clear that magnesium plays a vital role in biofilm formation and should be the focus of further investigations.

Magnesium is not only important for bacterial homeostasis but has also been found to inhibit induced autolysis in *E. coli* upon its addition (43). One mutant with a disruption of *mltD* produced low levels of biofilm in this screen. The membrane-bound lytic murein transglycosylase D precursor (*mltD*) encodes a murein-degrading enzyme (autolysin) and belongs to the class of lytic transglycosylases which are important for cell division and insertion of proteins in the cell envelope and also for the maintenance of bacterial morphology (44). Lytic transglycosylase activity on cell turnover has previously been linked to increased biofilm formation by Gram-negative (45, 46) and Gram-positive (47) bacteria. Cells in a biofilm are protected from exposure to exogenous toxic substances by the surrounding extracellular polymeric substance matrix within a heterogeneous metabolic bacterial population. By altering the cell structure, adhesion to surfaces and the ability of matrix production and anchoring is changed (48). Lamers et al. (49) showed that *mltD* mutants produced about 70% less biofilm than the wild-type *P. aeruginosa*. Similar results were observed by Sailer et al. (46) for *mltE* mutants of *E. coli*. In our study, *mtlD* mutants could possibly have suffered from interference with components of the cell membrane, possibly affecting the surface attachment, which is important for the initial steps of biofilm formation. However, we did not investigate the signaling pathway. It has been shown that a double mutation in two lytic transglycolase genes, *mltE* and *mltC*, was specifically linked to the regulation of biofilm formation by affecting the expression of the key biofilm gene regulator CsgD (45) in *Salmonella enterica* serovar Typhimurium. Another possible mechanism was proposed by Artola-Recolons et al. (50). The model involves the maturation of the surrounding peptidoglycan, via lytic transglycosylase, for the proper anchoring and functionality of the flagellar motor, which is required to allow successful colonization of the gastric mucosa by *H. pylori*.

In line with a previous finding (51), the *mltD* mutant produced elongated cells when assessed microscopically. The *mltD* mutant (39G5) was one of the few in the screen that exhibited no motility, which is in agreement with other studies (26, 27). Two other low biofilm formers with insertions in the *flaA* gene and a gene encoding an unknown protein (44F5) were also motility deficient (see Fig. S6), which might account for their low biofilm production. The successful complementation of the *mltD* mutant confirmed the gene's direct involvement in biofilm formation and motility. The reduction in motility and production of long chains with elongated cells might impair the ability of the mutant to move freely and to attach to surfaces, thus resulting in biofilm reduction. The observed lower autolysis rate after exposure of 39G5 to Triton X-100 was also seen in a previous study (51), further confirming the involvement of the *mltD* gene in autolysis.

Interestingly, the two genes influenced by magnesium in this study (*mgtB* and *mltD*) are both situated in very close proximity on the genome only 1,282 bp apart (see Fig. S3b). The coding region for *mltD* is situated on the positive strand and for *mgtB* on

the negative strand. A gene encoding a transcriptional regulator of the TetR family is situated between these two genes. *mltD* is suggested to be regulated by this gene (52), and TetR is known to be influenced by magnesium (53–55). The *mgtB* mutant (44D3) showed a low-biofilm phenotype, which was reversed to the wild-type level upon magnesium addition, whereas the *mltD* mutant (39G5) showed a further reduction in biofilm mass upon magnesium addition. This and the close proximity of the genes suggest a potential common regulatory mechanism, possibly through TetR, although different regulatory systems for the two genes have been suggested (35, 52); however, this needs to be further investigated.

This screen also identified a number of mutants with defects in cell wall and membrane functions that showed changes in biofilm formation. Of particular note, a transposon insertion in the *clsA* gene (34F11), encoding the cardiolipin synthetase, led to enhanced biofilm formation in the present study. Cardiolipin synthetase catalyzes the formation of cardiolipin from phosphatidylglycerol and is predominantly active in stationary phase (56). Previous research showed that gene disruption of *clsA* resulted in decreased biofilm formation by other Gram-negative and Gram-positive species (23–25), which indicates that *clsA* might be differentially regulated in different species, possibly due to differences in membrane composition. The hypothesis of differential regulation in multiple species is supported by studies which showed that changes in the environmental conditions, such as osmotic stress or desiccation, led to activation of *clsA* in *E. coli* and *Staphylococcus aureus* (57, 58), but butanol stress induced the downregulation of *clsA* in *B. subtilis* (59). By screening a mutant library of *L. monocytogenes* for desiccation survival, Hingston et al. (16) found that a transposon insertion in the gene *clsA* resulted in decreased desiccation survival compared to the wild type in *L. monocytogenes*.

Changes in environmental conditions not only trigger activation of genes involved in membrane composition to protect cells from damage but also trigger other stress response mechanisms. Many studies have shown that stress response is somehow linked to biofilm formation (11, 60–65). One well-described system is the SOS response which is induced upon replication fork stalling caused by DNA damage through reactive oxygen species (ROS) (66). UvrB is part of an enzyme complex that mediates excision and incision steps of DNA repair, and its expression is induced as part of the SOS response (67). In the present study, a gene disruption of *uvrB* resulted in a low-biofilm phenotype, although this phenotype could only be partially complemented. Partial complementation of *uvrB* may have occurred because this gene is part of an operon with *uvrA*, which may also have been affected by the transposon insertion (see Fig. S3b). The SOS response has been linked to biofilm formation by several bacterial species, including *L. monocytogenes*, *Pseudomonas aeruginosa*, and *Streptococcus mutans* (66–68). Gene expression of *uvrB* and stress response-associated genes was found to be upregulated in planktonic cells after heat exposure (69). Microscopic analysis of 33E11 showed changes in phenotype and produced coccoid-shaped bacteria (Fig. 3f). The formation of coccoid-shaped bacteria has been reported previously for *Listeria* cells after exposure to stresses such as starvation due to change from log growth to long-term survival (70, 71). Tremoulet et al. (72) found that the bacterial cells of 7-day-old biofilms of *L. monocytogenes* were more coccoid-shaped than rod-shaped, which agrees with our findings. The changes in phenotype might be due to maturation of the biofilm since these researchers did not observe this phenotype for biofilm grown for 24 h.

Although complementation was unsuccessful for the *clsA* and *mgtB* mutants in this study, their repeated identification in the screen, the different locations of the transposon insertions in these mutants, and in one instance the different orientation of the transposon (*clsA*) (Table 1) provided substantial evidence for their involvement in biofilm formation.

In addition, both *mgtB* mutants (30H2 and 44D3; Table 1) identified in this screen behaved similarly in the biofilm formation assay, in growth studies (see Fig. S1 and

Table S1) and in motility tests (see Fig. S6). The two *clsA* mutants (30A9 and 34F11) produced the same amount of biofilm and were also similar in growth behavior; however, they differed in motility. The higher motility for one of the *clsA* mutants (30A9) could be due to insertion locations producing a partially functional gene (30A9 [insertion after bp 1133] as opposed to bp 729 in 34F11). However, this will require further investigation.

Furthermore, the membrane protein cardiolipin is predominantly found at the cell poles of rod-shaped bacteria (73), and the lack of cardiolipin might affect incorporation or attachment of specific proteins, such as flagella, into the cell poles, resulting in decreased motility. A previous study found that the swimming motility of *Rhodobacter sphaeroides* was not affected by cardiolipin deficiency (23). However, in contrast to *L. monocytogenes*, which has four to six peritrichous flagella, *R. sphaeroides* has just one single flagellum and is usually not situated at the cell pole but medially on the cell body (74). This strengthens the evidence for the involvement of *clsA* in motility and perhaps indicates this only applies to peritrichous flagella.

The inability to restore the wild-type phenotypes in the *mgtB* and *clsA* mutants may have resulted from differential expression of the genes upon site-specific integration of the pIMK vector. This failure may also have been because of polar effects on the expression of downstream genes upon insertion of the transposon (see Fig. S3b). Certainly, the orientation of the transposon in the *mgtB* mutant suggests that the transposon could influence expression of downstream genes, such as *ftsW*, which are part of a cell division operon. However, together with literature linking these genes to biofilm formation in other studies (23, 38), their repeated identification provided strong evidence that they are somehow involved in biofilm formation by *L. monocytogenes* 15G01. A recent publication also found an interesting link between cardiolipin and MgtA (which belongs to the same transporter class as MgtB) in *E. coli*: both MgtA and cardiolipin were found together in the bacterial membrane. Subramani et al. (75) suggested that the head group of cardiolipin contributes to MgtA activation by possibly acting as a chaperone for MgtA. Whether a similar link is present in Gram-positive bacteria will need further investigation.

To conclude, two genes, *clsA* and *mgtB*, were identified as involved in biofilm formation. Both have not, to the best of our knowledge, been previously associated with biofilm formation by *L. monocytogenes*. The stress responsive gene *uvrB* is clearly part of an operon involved in biofilm formation, strengthening the link between biofilm formation and stress response. Confocal analysis revealed a unique biofilm structure for the *mgtB* mutant, which was reversed upon magnesium addition. Further studies analyzing gene regulation are required to assess the exact involvement of the biofilm-associated genes. Ultimately, this level of understanding could then help devise specific intervention technologies that reduce the tendency of these damaging foodborne pathogens to form such persistent biofilms.

MATERIALS AND METHODS

Bacterial strains and growth conditions. The wild-type strain used in this study was *L. monocytogenes* 15G01, a representative of the persistent pulsotype 5132 obtained from a New Zealand seafood-processing facility during an extensive sampling program (18). *L. monocytogenes* 15G01 was kept as glycerol stocks in a −80°C freezer and recovered in a three-step process by (i) growth in tryptic soy broth (TSB) enriched with 0.6% yeast extract (TSBYE; Difco, BD) overnight at 37°C, (ii) plating on tryptic soy agar enriched with 0.6% yeast extract (TSAYE; Difco, BD), and (iii) subculture and storage on Columbian sheep blood agar (Fort Richard, New Zealand) at 4°C. A library of 6,500 mutants of *L. monocytogenes* 15G01, created by The New Zealand Plant and Food Research Limited using the Himar1 mariner-based transposition system (22) according to a method described previously (76), was kept on 96-well master plates in glycerol at −80°C, subcultured twice before use, and stored on TSAYE plates supplemented with erythromycin (Duchefa, Biochemie, The Netherlands) at a final concentration of 5 ppm. Media and agar plates were supplemented with erythromycin at a final concentration of 5 ppm for the studies with the mutants (the transposon contains the erythromycin resistance gene) and with additional kanamycin (MP Biomedicals, Illkirch, France) at a concentration of 50 ppm for the complemented strains. The optical density measurements for the growth studies were taken at a wavelength of 595 or 600 nm using a microplate reader (Multiskan EX; Thermo Fisher) or an automated microplate reader (SPECTROstar Omega, BMG Labtech).

Biofilm formation assay. A biofilm formation assay was performed according to the method described by Djordjevic et al. (77) with some modifications. Briefly, overnight cultures were grown at 37°C in TSBYE in a sterile 96-well plate (polystyrene, U-bottom; Interlab, New Zealand) and transferred to new 96-well plates with a 96-well replicator, each well containing 200 μl of MWB (Himedia, India). The cultures were incubated for 48 h at 30°C and then washed three times with 200 μl of double-distilled H_2O (ddH_2O) using a microplate strip washer (ELx50; BioTek). After air-drying at ambient temperature for 30 min, 150 μl of a 1% aqueous crystal violet (CV) solution was added to the plates. After 45 min of incubation at 30°C, the CV solution was removed, and the cultures were washed six times with 150 μl of ddH_2O. After drying for 30 min at 30°C, 150 μl of 96% ethanol was added to each well to destain the CV-stained cells. The optical density was measured after 1 h at 595 nm with a microplate reader (Multiskan EX, Thermo Fisher). The OD_{595} values obtained were corrected by subtracting the OD_{595} value of sterile media. To screen the library of transposon mutants, mutants were stored in 96-well master-plates and subcultured twice before tests for biofilm formation. Biofilm formation for each mutant was measured three times and compared to the wild-type strain. Statistical analysis (two sample *t* test; $P \leq 0.05$) was performed to select mutants of interest. The OD_{595} values of the mutants selected for further analysis were at least two SD above or below that of the wild-type strain. To eliminate variability caused by growth deficiency, biofilm formation and turbidity measurements were repeated for 120 selected mutants in two independent experiments with eight replicates each. Turbidity was measured at 595 nm with a microplate reader before the washing and staining process. The growth of the mutants was compared to the growth of the wild type in MWB to confirm that the altered biofilm formation observed in the initial screen was not due to differences in the ability of the mutants to grow in this media (see Table S1 and Fig. S1).

To assess the influence of magnesium on biofilm formation, the CV assay was carried out in MWB with a final Mg^{2+} concentration of 1.67 or 5 mM, respectively. Biofilm formation was measured at 30 and 37°C for 48 h.

Identification of transposon insertion sites in selected mutants. To locate the transposon insertion sites in the genomes of the mutants of interest, a nested arbitrary PCR was performed using one transposon specific primer and one arbitrary primer (Table 4) to amplify the regions flanking the transposon from the right and the left end. The PCR was performed in two steps with the Mastercycler gradient (Eppendorf, Germany). BioMix Red (Bioline, UK) was used as the mastermix in the first round and the second round was run using AccuPrime Hifi *Taq* polymerase (Invitrogen, USA) as described previously (22). The annealing temperature was adjusted for each mutant, if necessary, to minimize nonspecific annealing or to increase annealing. A final concentration of 3 mM Mg^{2+} was used for all PCRs. A portion (5 μl) of each amplified product was visualized on a 1.5% agarose gel (settings, 100 V for 30 min) using Redsafe (Intron Biotechnology, South Korea) under UV light. The PCR products obtained were subsequently purified and sequenced by Macrogen, Ltd. (South Korea) and analyzed using the NCBI BLAST program, version 2.2.30 (available from https://www.ncbi.nlm.nih.gov), and the Geneious 7 program (78). The reference strain *L. monocytogenes* EGD (accession HG421741) (79) was used to identify the coordinates at the point of the transposon insertion site and the orientation of the transposon in the chromosome. This reference strain was chosen since it is the same serotype as the *L. monocytogenes* 15G01 strain (1/2a).

Complementation of selected mutants. The site-specific integrative vector pIMK (80) was used for the genetic complementation of selected mutants. The vector pIMK is a derivative of pPL2 (1 kb smaller) and facilitates the insertion at the $tRNA_{Arg}$ locus (81). Genetic complementation constructs using this plasmid were constructed by amplifying the target genes from wild-type 15G01 using gene-specific primers in PCR (Table 4). The gene-specific PCR products and the pIMK vector were digested with PstI and BamHI and ligated to one another using the LigaFast rapid DNA ligation system (Promega), following the manufacturer's instructions, in a molar ratio 3:1 (vector to insert). A 1-μl portion of the recombinant plasmid was then introduced into chemically competent *E. coli* S17 cells by heat shock. Transformants were selected on Luria-Bertani (LB) agar plates supplemented with kanamycin. A colony was picked from the agar plate with a sterile toothpick and dipped in the PCR mix. Colony PCR was performed with one gene-specific primer and T7 (T7 binding site present in the pIMK plasmid) to confirm successful transformation. Recombinant plasmids were extracted from colony PCR-positive cultures, and the gene inserts were sequenced to confirm the authenticity of the constructs. Authentic transformants were then used for the genetic complementation of *L. monocytogenes* 15G01 mutants. Conjugation was performed according to Azizoglu et al. (82) with some modifications. Single colonies of the donor (*E. coli* transformants containing the construct pIMK:gene or a control containing only the pIMK vector) were resuspended overnight in LB broth containing kanamycin and incubated at 30°C at 100 rpm to an OD_{595} of ~0.55. At the same time, a colony of the recipient (*L. monocytogenes* 15G01 transposon mutant) was resuspended in brain-heart infusion (BHI; Difco, BD) medium and incubated overnight at 37°C with shaking. The donor culture (3 ml) and a prewarmed (45°C; 10 min) recipient culture (1.5 ml) were mixed and centrifuged at 2,050 $\times$ *g* for 8 min; the bacterial pellet was then washed with 10 ml of BHI broth and centrifuged again under the same conditions. After a washing step, the pellet was resuspended in 500 μl of fresh BHI broth, deposited in the center of a BHI agar plate, and incubated overnight at 37°C. The drop was then resuspended in 2 ml of BHI broth, and a 100-μl aliquot was spread plated on BHI agar plates containing kanamycin and nalidixic acid (Fort Richard, New Zealand) (20 μg/ml). *L. monocytogenes* strains are naturally resistant against nalidixic acid, and therefore it was used for counterselection. The plates were incubated at 30°C for 2 to 3 days. The authenticity of transconjugants was confirmed by colony PCR using the corresponding gene-specific primers. Their identity as *L. monocytogenes* was also confirmed using 16S-rRNA specific primers for *L. monocytogenes* (Table 4). To confirm that the empty vector

TABLE 4 Primers used in this study

Usage and primer	Primer nucleotide sequence (5′–3′)[a]	Product size (bp)	Source or reference
Complementation of 33E11			
uvrB_Fwd	CAA*CTGCAG*CCTTCAATTAAATCCACATCTGGT (PstI)	2,528	This study
uvrB_Rev	AAC*GGATCC*TGTGCTTGCAACGTATATGCT (BamHI)		This study
Complementation of 39G5			
mltD_Fwd	CAA*CTGCAG*TTGACGTAGAAACACCTTAGCAC (PstI)	2,683	This study
mltD_ Rev	AAC*GGATCC*AAAGGCAATTTCGGTGCGAC (BamHI)		This study
Identification of *L. monocytogenes*			
16S_Fwd	CAGCAGCCGCGGTAATAC	938	87
16S_Rev	CTCCATAAAGGTGACCCT		87
Arbitrary PCR			
Marq254	CGTGGAATACGGGTTTGCTAAAAG		76
Marq255	CAGTACAATCTGCTCTGATGCCGCATAGTT		76
Marq206	TGTCAGACATATGGGCACACGAAAAACAAGT		76
Marq207	GGCCACGCGTCGACTAGTACNNNNNNNNNNGTAAT		76
Marq208	GGCCACGCGTCGACTAGTAC		76
Marq257	CTTACAGACAAGCTGTGACCGTCT		76
Marq270	TGTGAAATACCGCACAGATGCGAAGGGCGA		76
Marq271	GGGAATCATTTGAAGGTTGGTACT		76
Presence of vector pIMK			
T7promoter	TAATACGACTCACTATAGGG		Macrogen, Inc. (South Korea)

[a]Italics represent restriction enzyme sites; the restriction enzymes used are indicated in parentheses. N = A, C, G, or T.

had no effect on the phenotype, the parent plasmid was transformed in each mutant, as well as in the wild-type strain 15G01.

Microscopic analysis. Fluorescence microscopy, scanning electron microscopy (SEM), and confocal laser scanning microscopy were used to visualize biofilm formation by bacterial strains on polystyrene, stainless steel, and glass, respectively. For visualization under fluorescence, a fluorescent Live/Dead *Bac*Light bacterial viability kit (Life Technologies, Thermo Fisher, New Zealand) was used to label living cells green (SYTO9, membrane-permeable stain) and dead cells red (propidium iodide, a non-membrane-permeable stain). Six-well plates (tissue treated; Greiner, Germany) were filled with 2.97 ml of MWB, inoculated with 30 μl of an overnight bacterial culture grown in TSBYE at 37°C, and incubated at 30°C for 48 h. The biofilms were then washed twice with 0.8% NaCl to remove loosely attached cells and stained with 1 ml of fluorescent stain prepared according to the manufacturer's manual. A fluorescence microscope (Olympus, BX51 fitted with the XC30 digital camera) was used at 10 $\times$ 100 magnification to take images.

SEM was performed on stainless steel coupons (5 $\times$ 5 mm, food grade) as described previously (83). The coupons were coated with cooked mussel juice (CMJ) produced as described previously (19), but with some modifications. Briefly, Greenshell mussels obtained from the local supermarket were stored for 24 h at 10°C in a fridge and then boiled in a wok closed with a lid without the addition of water. When all mussels opened and released the intervalvular juice, the liquid was collected and autoclaved at 121°C for 15 min. The coupons were pretreated with alkali detergent for 2 h at 45°C, rinsed with ddH_2O, and autoclaved in deionized water. The coupons were coated by immersion in CMJ in a 6-well plate (tissue treated, Greiner, Germany) for 4 h at 60°C (or until dried). The coupons were then placed into a fresh 6-well plate containing MWB (2.97 ml) and inoculated with 30 μl of an overnight culture of the bacterium ($10^{7.5}$ to 10^8 CFU). After incubation for 7 days at 30°C, phosphate-buffered saline (PBS; pH 7.2) was used to remove loosely attached cells on the coupons. After a rinse with 100 mM cacodylate buffer (pH 7.2; Acros Organics, NJ), the coupons were fixed overnight at 4°C in 2% glutaraldehyde (Acros Organics, NJ) and 0.1% ruthenium red solution (Acros Organics) in 100 mM cacodylate buffer. The next morning, coupons were rinsed to remove unbound dye and then dehydrated in serial dilutions of ethanol for 10 min each (30, 50, 60, 70, and 90% [vol/vol]) with three final 10-min rinses in absolute ethanol. The coupons were then critical point dried (BalTec CPD030; BalTec AG, Balzers, Liechtenstein) and sputter coated with gold (Leica EM ACE200; Leica Microscopy Systems Ltd., Heerbrugg, Switzerland) for visualization using a scanning electron microscope (FEI Quanta 250 SEM; Fei Company, Hillsboro, OR).

For confocal laser scanning microscopy (CLSM) analysis, the biofilms were grown on glass-bottom dishes (35-mm petri dish, 10-mm Microwell no. 0 coverglass; MatTek Corporation). First, single colonies picked from an agar plate (TSAYE) were used to inoculate TSBYE and then incubated overnight at 37°C. The glass-bottom dishes were filled with 2.97 ml of MWB (Mg^{2+} concentration 1.67 or 5 mM) and inoculated with 30 μl of the overnight culture. After 7 days of incubation at 30°C (or 37°C for 39G5), the medium was carefully removed, and the biofilm on the plates washed twice with 0.8% NaCl solution. The fluorescent Live/Dead *Bac*Light bacterial viability kit was used to stain the biofilms according to the manufacturer's instructions. Three images (246.03 $\times$ 246.03 μm) per sample were taken with a Leica

DM6000B scanning confocal microscope running LAS AF software version 2.7.3.9723. Excitation and emission levels were as follows: (i) SYTO9 stain, excitation at 488 nm (argon laser) and emission collection at 498 to 550 nm, and (ii) propidium iodide stain, excitation at 561 nm (DPSS 561 laser) and emission collection at 571 to 700 nm.

Images were analyzed using ImageJ software and/or Imaris (Bitplane, Zurich). COMSTAT (www.comstat.dk) was used to calculate the biomass, roughness, and maximum and average thicknesses of the biofilms (84, 85).

Motility assay. A motility assay was performed according to the method of Knudsen et al. (86). Briefly, semisolid agar plates (TSB plus 0.25% agar [Difco, BD]) were inoculated with *L. monocytogenes* 15G01 or the mutant (39G5) using a sterile pick and then incubated at 30 or 37°C for 48 h. The diameter of the halo formed around the colony was then measured and compared to the halo surrounding the wild-type strain (15G01). Three independent experiments were performed with each treatment repeated in triplicate.

Autolysis assay. The assay was performed according to Huang et al. (10) with minor modifications. Briefly, single colonies of the wild type and the selected mutant (39G5) were picked from the TSAYE plate and grown in BHI at 37°C overnight. OD_{595} was measured in a microplate reader (SPECTROstar Omega; BMG Labtech) and adjusted to 0.6 ± 0.05 for each culture. Each culture (1.5 ml) was transferred to 2-ml microtubes and centrifuged at 4°C at 4,500 $\times$ *g* for 10 min. The supernatant was discarded, and the cell pellet washed twice with ice-cold ddH_2O and then resuspended in the same volume of Tris-HCl (pH 7.2) containing 0.05% Triton X-100. Solutions with cells were incubated at 30°C in a 96-well plate, and the OD_{595} was measured for 20 h in 5-min intervals using an automated microplate reader (SPECTROstar Omega).

Data availability. The data that support the findings of this study are available from the corresponding author upon reasonable request (sandra.visnovsky@plantandfood.co.nz).

SUPPLEMENTAL MATERIAL

Supplemental material is available online only.

SUPPLEMENTAL FILE 1, PDF file, 0.7 MB.

ACKNOWLEDGMENTS

We thank Erik Rikkerink and Falk Kalamorz for valuable feedback on the manuscript, Duncan Hedderley for help with the statistical analysis, and Ian Hallett and Paul Sutherland for help with the SEM.

This research was funded through The New Zealand Ministry of Business, Innovation, and Employment (MBIE) funding under contract CAWX1801.

The authors declare that there are no conflicts of interest and that the research does not involve human participants and/or animals.

REFERENCES

1. Rocourt J, Jacquet C, Reilly A. 2000. Epidemiology of human listeriosis and seafoods. Int J Food Microbiol 62:197–209. https://doi.org/10.1016/S0168-1605(00)00336-6.
2. Lecuit M. 2005. Understanding how *Listeria monocytogenes* targets and crosses host barriers. Clin Microbiol Infect 11:430–436. https://doi.org/10.1111/j.1469-0691.2005.01146.x.
3. Fletcher G, Rogers M, Wong R. 1994. Survey of *Listeria monocytogenes* in New Zealand seafood. J Aquat Food Prod 3:13–24. https://doi.org/10.1300/J030v03n02_03.
4. Gudbjörnsdóttir B, Suihko ML, Gustavsson P, Thorkelsson G, Salo S, Sjöberg AM, Niclasen O, Bredholt S. 2004. The incidence of *Listeria monocytogenes* in meat, poultry and seafood plants in the Nordic countries. Food Microbiol 21:217–225. https://doi.org/10.1016/S0740-0020(03)00012-1.
5. Srey S, Jahid IK, Ha S-D. 2013. Biofilm formation in food industries: a food safety concern. Food Control 31:572–585. https://doi.org/10.1016/j.foodcont.2012.12.001.
6. Lou Y, Yousef AE. 1999. Characteristics of *Listeria monocytogenes* important to food processors, p 131–224. *In* Ryser ET, Marth EH (ed), *Listeria*, listeriosis, and food safety, 2nd ed. Marcel Dekker, New York, NY.
7. Carpentier B, Cerf O. 2011. Review: persistence of *Listeria monocytogenes* in food industry equipment and premises. Int J Food Microbiol 145:1–8. https://doi.org/10.1016/j.ijfoodmicro.2011.01.005.
8. Cruz CD, Fletcher GC. 2012. Assessing manufacturers' recommended concentrations of commercial sanitizers on inactivation of *Listeria monocytogenes*. Food Control 26:194–199. https://doi.org/10.1016/j.foodcont.2012.01.041.
9. Van Houdt R, Michiels CW. 2010. Biofilm formation and the food industry, a focus on the bacterial outer surface. J Appl Microbiol 109:1117–1131. https://doi.org/10.1111/j.1365-2672.2010.04756.x.
10. Huang Y, Shi C, Yu S, Li K, Shi X. 2012. A putative MerR family regulator involved in biofilm formation in *Listeria monocytogenes* 4b G. Foodborne Pathog Dis 9:767–772. https://doi.org/10.1089/fpd.2011.1101.
11. Huang Y, Suo Y, Shi C, Szlavik J, Shi XM, Knochel S. 2013. Mutations in *gltB* and *gltC* reduce oxidative stress tolerance and biofilm formation in *Listeria monocytogenes* 4b G. Int J Food Microbiol 163:223–230. https://doi.org/10.1016/j.ijfoodmicro.2013.02.023.
12. Alonso AN, Perry KJ, Regeimbal JM, Regan PM, Higgins DE. 2014. Identification of *Listeria monocytogenes* determinants required for biofilm formation. PLoS One 9:e113696. https://doi.org/10.1371/journal.pone.0113696.
13. Chang Y, Gu W, Fischer N, McLandsborough L. 2012. Identification of genes involved in *Listeria monocytogenes* biofilm formation by mariner-based transposon mutagenesis. Appl Microbiol Biotechnol 93:2051–2062. https://doi.org/10.1007/s00253-011-3719-z.
14. Ouyang Y, Li J, Dong Y, Blakely LV, Cao M. 2012. Genome-wide screening of genes required for *Listeria monocytogenes* biofilm formation. J Biotech Res 4:13–25.
15. Piercey MJ, Hingston PA, Truelstrup Hansen L. 2016. Genes involved in *Listeria monocytogenes* biofilm formation at a simulated food processing plant temperature of 15°C. Int J Food Microbiol 223:63–74. https://doi.org/10.1016/j.ijfoodmicro.2016.02.009.
16. Hingston PA, Piercey MJ, Truelstrup Hansen L. 2015. Genes associated with desiccation and osmotic stress in *Listeria monocytogenes* as revealed

by insertional mutagenesis. Appl Environ Microbiol 81:5350–5362. https://doi.org/10.1128/AEM.01134-15.
17. Collins B, Joyce S, Hill C, Cotter PD, Ross RP. 2010. TelA contributes to the innate resistance of *Listeria monocytogenes* to nisin and other cell wall-acting antibiotics. Antimicrob Agents Chemother 54:4658–4663. https://doi.org/10.1128/AAC.00290-10.
18. Cruz CD, Fletcher GC. 2011. Prevalence and biofilm-forming ability of *Listeria monocytogenes* in New Zealand mussel (*Perna canaliculus*) processing plants. Food Microbiol 28:1387–1393. https://doi.org/10.1016/j.fm.2011.06.014.
19. Nowak J, Cruz CD, Palmer J, Fletcher GC, Flint S. 2015. Biofilm formation of the *L. monocytogenes* strain 15G01 is influenced by changes in environmental conditions. J Microbiol Methods 119:189–195. https://doi.org/10.1016/j.mimet.2015.10.022.
20. Nowak J, Cruz CD, Tempelaars M, Abee T, van Vliet AHM, Fletcher GC, Hedderley D, Palmer J, Flint S. 2017. Persistent *Listeria monocytogenes* strains isolated from mussel production facilities form more biofilm but are not linked to specific genetic markers. Int J Food Microbiol 256:45–53. https://doi.org/10.1016/j.ijfoodmicro.2017.05.024.
21. Cruz CD, Pitman AR, Harrow SA, Fletcher GC. 2014. *Listeria monocytogenes* associated with New Zealand seafood production and clinical cases: unique sequence types, truncated InlA, and attenuated invasiveness. Appl Environ Microbiol 80:1489–1497. https://doi.org/10.1128/AEM.03305-13.
22. Nowak J, Visnovsky S, Cruz CD, Fletcher G, van Vliet AHM, Hedderley D, Butler R, Flint S, Palmer J, Pitman A. 2021. Inactivation of the gene encoding the cationic antimicrobial peptide resistance factor MprF increases biofilm formation but reduces invasiveness of *Listeria monocytogenes*. J Appl Microbiol 130:464–467. https://doi.org/10.1111/jam.14790.
23. Lin TY, Santos TM, Kontur WS, Donohue TJ, Weibel DB. 2015. A cardiolipin-deficient mutant of *Rhodobacter sphaeroides* has an altered cell shape and is impaired in biofilm formation. J Bacteriol 197:3446–3455. https://doi.org/10.1128/JB.00420-15.
24. Munoz-Elias EJ, Marcano J, Camilli A. 2008. Isolation of *Streptococcus pneumoniae* biofilm mutants and their characterization during nasopharyngeal colonization. Infect Immun 76:5049–5061. https://doi.org/10.1128/IAI.00425-08.
25. Puttamreddy S, Cornick NA, Minion FC. 2010. Genome-wide transposon mutagenesis reveals a role for pO157 genes in biofilm development in *Escherichia coli* O157:H7 EDL933. Infect Immun 78:2377–2384. https://doi.org/10.1128/IAI.00156-10.
26. Machata S, Hain T, Rohde M, Chakraborty T. 2005. Simultaneous deficiency of both MurA and p60 proteins generates a rough phenotype in *Listeria monocytogenes*. J Bacteriol 187:8385–8394. https://doi.org/10.1128/JB.187.24.8385-8394.2005.
27. Machata S. 2008. Molecular investigations of peptidoglycan-binding proteins in Listeria monocytogenes. PhD thesis. Justus-Liebig-Universitaet Giessen, Giessen, Germany.
28. Bao Y, Zhang X, Jiang Q, Xue T, Sun B. 2015. Pfs promotes autolysis-dependent release of eDNA and biofilm formation in *Staphylococcus aureus*. Med Microbiol Immunol 204:215–226. https://doi.org/10.1007/s00430-014-0357-y.
29. Webb AJ, Karatsa-Dodgson M, Grundling A. 2009. Two-enzyme systems for glycolipid and polyglycerolphosphate lipoteichoic acid synthesis in *Listeria monocytogenes*. Mol Microbiol 74:299–314. https://doi.org/10.1111/j.1365-2958.2009.06829.x.
30. Parsek MR, Fuqua C. 2004. Biofilms 2003: emerging themes and challenges in studies of surface-associated microbial life. J Bacteriol 186:4427–4440. https://doi.org/10.1128/JB.186.14.4427-4440.2004.
31. Mulcahy H, Lewenza S. 2011. Magnesium limitation is an environmental trigger of the *Pseudomonas aeruginosa* biofilm lifestyle. PLoS One 6:e23307. https://doi.org/10.1371/journal.pone.0023307.
32. Kehres DG, Maguire ME. 2003. The unusual nature of magnesium transporters, p 347–360. *In* Microbial transport systems. Wiley-VCH Verlag GmbH & Co., Berlin, Germany.
33. Chamnongpol S, Groisman EA. 2002. Mg^{2+} homeostasis and avoidance of metal toxicity. Mol Microbiol 44:561–571. https://doi.org/10.1046/j.1365-2958.2002.02917.x.
34. Groisman EA, Cromie MJ, Shi Y, Latifi T. 2006. A Mg^{2+}-responding RNA that controls the expression of a Mg^{2+} transporter. Cold Spring Harbor Symp Quant Biol 71:251–258. https://doi.org/10.1101/sqb.2006.71.005.
35. Nielsen PK, Andersen AZ, Mols M, van der Veen S, Abee T, Kallipolitis BH. 2012. Genome-wide transcriptional profiling of the cell envelope stress response and the role of LisRK and CesRK in *Listeria monocytogenes*. Microbiology (Reading) 158:963–974. https://doi.org/10.1099/mic.0.055467-0.
36. Kallipolitis BH, Ingmer H, Gahan CG, Hill C, Søgaard-Andersen L. 2003. CesRK, a two-component signal transduction system in *Listeria monocytogenes*, responds to the presence of cell wall-acting antibiotics and affects β-lactam resistance. Antimicrob Agents Chemother 47:3421–3429. https://doi.org/10.1128/AAC.47.11.3421-3429.2003.
37. Gottschalk S, Bygebjerg-Hove I, Bonde M, Nielsen PK, Nguyen TH, Gravesen A, Kallipolitis BH. 2008. The two-component system CesRK controls the transcriptional induction of cell envelope-related genes in *Listeria monocytogenes* in response to cell wall-acting antibiotics. J Bacteriol 190:4772–4776. https://doi.org/10.1128/JB.00015-08.
38. Hartmann I, Carranza P, Lehner A, Stephan R, Eberl L, Riedel K. 2010. Genes involved in *Cronobacter sakazakii* biofilm formation. Appl Environ Microbiol 76:2251–2261. https://doi.org/10.1128/AEM.00930-09.
39. Coffey BM, Akhand SS, Anderson GG. 2014. MgtE is a dual-function protein in *Pseudomonas aeruginosa*. Microbiology (Reading) 160:1200–1213. https://doi.org/10.1099/mic.0.075275-0.
40. Guilbaud M, Piveteau P, Desvaux M, Brisse S, Briandet R. 2015. Exploring the diversity of *Listeria monocytogenes* biofilm architecture by high-throughput confocal laser scanning microscopy and the predominance of the honeycomb-like morphotype. Appl Environ Microbiol 81:1813–1819. https://doi.org/10.1128/AEM.03173-14.
41. Oknin H, Steinberg D, Shemesh M. 2015. Magnesium ions mitigate biofilm formation of Bacillus species via downregulation of matrix genes expression. Front Microbiol 6:907. https://doi.org/10.3389/fmicb.2015.00907.
42. Song B, Leff LG. 2006. Influence of magnesium ions on biofilm formation by *Pseudomonas fluorescens*. Microbiol Res 161:355–361. https://doi.org/10.1016/j.micres.2006.01.004.
43. Leduc M, Kasra R, van Heijenoort J. 1982. Induction and control of the autolytic system of *Escherichia coli*. J Bacteriol 152:26–34.
44. Scheurwater E, Reid CW, Clarke AJ. 2008. Lytic transglycosylases: bacterial space-making autolysins. Int J Biochem Cell Biol 40:586–591. https://doi.org/10.1016/j.biocel.2007.03.018.
45. Monteiro C, Fang X, Ahmad I, Gomelsky M, Römling U. 2011. Regulation of biofilm components in *Salmonella enterica* serovar Typhimurium by lytic transglycosylases involved in cell wall turnover. J Bacteriol 193:6443–6451. https://doi.org/10.1128/JB.00425-11.
46. Sailer FC, Meberg BM, Young KD. 2003. β-Lactam induction of colanic acid gene expression in *Escherichia coli*. FEMS Microbiol Lett 226:245–249. https://doi.org/10.1016/S0378-1097(03)00616-5.
47. Kolar SL, Nagarajan V, Oszmiana A, Rivera FE, Miller HK, Davenport JE, Riordan JT, Potempa J, Barber DS, Koziel J, Elasri MO, Shaw LN. 2011. NsaRS is a cell-envelope-stress-sensing two-component system of *Staphylococcus aureus*. Microbiology (Reading) 157:2206–2219. https://doi.org/10.1099/mic.0.049692-0.
48. Bucher T, Oppenheimer-Shaanan Y, Savidor A, Bloom-Ackermann Z, Kolodkin A, Gal I. 2015. Disturbance of the bacterial cell wall specifically interferes with biofilm formation. Environ Microbiol Rep 7:990–1004. https://doi.org/10.1111/1758-2229.12346.
49. Lamers RP, Nguyen UT, Nguyen Y, Buensuceso RN, Burrows LL. 2015. Loss of membrane-bound lytic transglycosylases increases outer membrane permeability and β-lactam sensitivity in *Pseudomonas aeruginosa*. Microbiologyopen 4:879–895. https://doi.org/10.1002/mbo3.286.
50. Artola-Recolons C, Lee M, Bernardo-García N, Blázquez B, Hesek D, Bartual SG, Mahasenan KV, Lastochkin E, Pi H, Boggess B, Meindl K, Usón I, Fisher JF, Mobashery S, Hermoso JA. 2014. Structure and cell wall cleavage by modular lytic transglycosylase MltC of *Escherichia coli*. ACS Chem Biol 9:2058–2066. https://doi.org/10.1021/cb500439c.
51. Carroll SA, Hain T, Technow U, Darji A, Pashalidis P, Joseph SW, Chakraborty T. 2003. Identification and characterization of a peptidoglycan hydrolase, MurA, of *Listeria monocytogenes*, a muramidase needed for cell separation. J Bacteriol 185:6801–6808. https://doi.org/10.1128/JB.185.23.6801-6808.2003.
52. Chatterjee SS, Hossain H, Otten S, Kuenne C, Kuchmina K, Machata S, Domann E, Chakraborty T, Hain T. 2006. Intracellular gene expression profile of *Listeria monocytogenes*. Infect Immun 74:1323–1338. https://doi.org/10.1128/IAI.74.2.1323-1338.2006.
53. Leypold CF, Marian DT, Roman C, Schneider S, Schubert P, Scholz O, Hillen W, Clark T, Lanig H. 2004. How does Mg^{2+} affect the binding of anhydrotetracycline in the TetR protein? Photochem Photobiol Sci 3:109–119. https://doi.org/10.1039/b303431n.
54. Scholz O, Schubert P, Kintrup M, Hillen W. 2000. Tet repressor induction without Mg^{2+}. Biochem 39:10914–10920. https://doi.org/10.1021/bi001018p.

55. Werten S, Dalm D, Palm GJ, Grimm CC, Hinrichs W. 2014. Tetracycline repressor allostery does not depend on divalent metal recognition. Biochemistry 53:7990–7998. https://doi.org/10.1021/bi5012805.
56. Koprivnjak T, Zhang D, Ernst CM, Peschel A, Nauseef WM, Weiss JP. 2011. Characterization of *Staphylococcus aureus* cardiolipin synthases 1 and 2 and their contribution to accumulation of cardiolipin in stationary phase and within phagocytes. J Bacteriol 193:4134–4142. https://doi.org/10.1128/JB.00288-11.
57. Maudsdotter L, Imai S, Ohniwa RL, Saito S, Morikawa K. 2015. *Staphylococcus aureus* dry stress survivors have a heritable fitness advantage in subsequent dry exposure. Microbes Infect 17:456–461. https://doi.org/10.1016/j.micinf.2015.02.004.
58. Romantsov T, Guan Z, Wood JM. 2009. Cardiolipin and the osmotic stress responses of bacteria. Biochim Biophys Acta 1788:2092–2100. https://doi.org/10.1016/j.bbamem.2009.06.010.
59. Vinayavekhin N, Mahipant G, Vangnai AS, Sangvanich P. 2015. Untargeted metabolomics analysis revealed changes in the composition of glycerolipids and phospholipids in *Bacillus subtilis* under 1-butanol stress. Appl Microbiol Biotechnol 99:5971–5983. https://doi.org/10.1007/s00253-015-6692-0.
60. Suo Y, Huang Y, Liu Y, Shi C, Shi X. 2012. The expression of superoxide dismutase (SOD) and a putative ABC transporter permease is inversely correlated during biofilm formation in *Listeria monocytogenes* 4b G. PLoS One 7:e48467. https://doi.org/10.1371/journal.pone.0048467.
61. Taylor CM, Beresford M, Epton HA, Sigee DC, Shama G, Andrew PW, Roberts IS. 2002. *Listeria monocytogenes relA* and *hpt* mutants are impaired in surface-attached growth and virulence. J Bacteriol 184:621–628. https://doi.org/10.1128/JB.184.3.621-628.2002.
62. van der Veen S, Abee T. 2010. Dependence of continuous-flow biofilm formation by *Listeria monocytogenes* EGD-e on SOS response factor YneA. Appl Environ Microbiol 76:1992–1995. https://doi.org/10.1128/AEM.02680-09.
63. van der Veen S, Abee T. 2010. HrcA and DnaK are important for static and continuous-flow biofilm formation and disinfectant resistance in *Listeria monocytogenes*. Microbiology (Reading) 156:3782–3790. https://doi.org/10.1099/mic.0.043000-0.
64. van der Veen S, Abee T. 2010. Importance of SigB for *Listeria monocytogenes* static and continuous-flow biofilm formation and disinfectant resistance. Appl Environ Microbiol 76:7854–7860. https://doi.org/10.1128/AEM.01519-10.
65. van der Veen S, Abee T. 2011. Generation of variants in *Listeria monocytogenes* continuous-flow biofilms is dependent on radical-induced DNA damage and RecA-mediated repair. PLoS One 6:e28590. https://doi.org/10.1371/journal.pone.0028590.
66. van der Veen S, Abee T. 2011. Bacterial SOS response: a food safety perspective. Curr Opin Biotechnol 22:136–142. https://doi.org/10.1016/j.copbio.2010.11.012.
67. van der Veen S, van Schalkwijk S, Molenaar D, de Vos WM, Abee T, Wells-Bennik MH. 2010. The SOS response of *Listeria monocytogenes* is involved in stress resistance and mutagenesis. Microbiology (Reading) 156:374–384. https://doi.org/10.1099/mic.0.035196-0.
68. Inagaki S, Matsumoto-Nakano M, Fujita K, Nagayama K, Funao J, Ooshima T. 2009. Effects of recombinase A deficiency on biofilm formation by *Streptococcus mutans*. Oral Microbiol Immunol 24:104–108. https://doi.org/10.1111/j.1399-302X.2008.00480.x.
69. van der Veen S, Hain T, Wouters JA, Hossain H, de Vos WM, Abee T, Chakraborty T, Wells-Bennik MH. 2007. The heat-shock response of *Listeria monocytogenes* comprises genes involved in heat shock, cell division, cell wall synthesis, and the SOS response. Microbiology (Reading) 153:3593–3607. https://doi.org/10.1099/mic.0.2007/006361-0.
70. Doijad SP, Barbuddhe SB, Garg S, Poharkar KV, Kalorey DR, Kurkure NV, Rawool DB, Chakraborty T. 2015. Biofilm-forming abilities of *Listeria monocytogenes* serotypes isolated from different sources. PLoS One 10:e0137046. https://doi.org/10.1371/journal.pone.0137046.
71. Wen J, Anantheswaran RC, Knabel SJ. 2009. Changes in barotolerance, thermotolerance, and cellular morphology throughout the life cycle of *Listeria monocytogenes*. Appl Environ Microbiol 75:1581–1588. https://doi.org/10.1128/AEM.01942-08.
72. Tremoulet F, Duche O, Namane A, Martinie B, Labadie JC, European Listeria Genome Consortium. 2002. Comparison of protein patterns of *Listeria monocytogenes* grown in biofilm or in planktonic mode by proteomic analysis. FEMS Microbiol Lett 210:25–31. https://doi.org/10.1016/S0378-1097(02)00571-2.
73. Dworkin J. 2009. Cellular polarity in prokaryotic organisms. Cold Spring Harb Perspect Biol 1:a003368. https://doi.org/10.1101/cshperspect.a003368.
74. Armitage JP, Macnab RM. 1987. Unidirectional, intermittent rotation of the flagellum of *Rhodobacter sphaeroides*. J Bacteriol 169:514–518. https://doi.org/10.1128/JB.169.2.514-518.1987.
75. Subramani S, Perdreau-Dahl H, Morth JP. 2016. The magnesium transporter A is activated by cardiolipin and is highly sensitive to free magnesium *in vitro*. Elife 5:e11407. https://doi.org/10.7554/eLife.11407.
76. Cao M, Bitar AP, Marquis H. 2007. A mariner-based transposition system for *Listeria monocytogenes*. Appl Environ Microbiol 73:2758–2761. https://doi.org/10.1128/AEM.02844-06.
77. Djordjevic D, Wiedmann M, McLandsborough LA. 2002. Microtiter plate assay for assessment of *Listeria monocytogenes* biofilm formation. Appl Environ Microbiol 68:2950–2958. https://doi.org/10.1128/AEM.68.6.2950-2958.2002.
78. Kearse M, Moir R, Wilson A, Stones-Havas S, Cheung M, Sturrock S, Buxton S, Cooper A, Markowitz S, Duran C, Thierer T, Ashton B, Meintjes P, Drummond A. 2012. Geneious Basic: an integrated and extendable desktop software platform for the organization and analysis of sequence data. Bioinformatics 28:1647–1649. https://doi.org/10.1093/bioinformatics/bts199.
79. Becavin C, Bouchier C, Lechat P, Archambaud C, Creno S, Gouin E, Wu Z, Kuhbacher A, Brisse S, Pucciarelli MG, Garcia-del Portillo F, Hain T, Portnoy DA, Chakraborty T, Lecuit M, Pizarro-Cerda J, Moszer I, Bierne H, Cossart P. 2014. Comparison of widely used *Listeria monocytogenes* strains EGD, 10403S, and EGD-e highlights genomic variations underlying differences in pathogenicity. mBio 5:e00969-14. https://doi.org/10.1128/mBio.00969-14.
80. Monk IR, Gahan CG, Hill C. 2008. Tools for functional postgenomic analysis of listeria monocytogenes. Appl Environ Microbiol 74:3921–3934. https://doi.org/10.1128/AEM.00314-08.
81. Lauer P, Chow MY, Loessner MJ, Portnoy DA, Calendar R. 2002. Construction, characterization, and use of two *Listeria monocytogenes* site-specific phage integration vectors. J Bacteriol 184:4177–4186. https://doi.org/10.1128/JB.184.15.4177-4186.2002.
82. Azizoglu RO, Elhanafi D, Kathariou S. 2014. Mutant construction and integration vector-mediated gene complementation in *Listeria monocytogenes*. Methods Mol Biol 1157:201–211. https://doi.org/10.1007/978-1-4939-0703-8_17.
83. Borucki MK, Peppin JD, White D, Loge F, Call DR. 2003. Variation in biofilm formation among strains of *Listeria monocytogenes*. Appl Environ Microbiol 69:7336–7342. https://doi.org/10.1128/AEM.69.12.7336-7342.2003.
84. Heydorn A, Nielsen AT, Hentzer M, Sternberg C, Givskov M, Ersboll BK, Molin S. 2000. Quantification of biofilm structures by the novel computer program COMSTAT. Microbiol (Reading) 146:2395–2407. https://doi.org/10.1099/00221287-146-10-2395.
85. Vorregaard M. 2008. Comstat2: a modern 3D image analysis environment for biofilms. Technical University of Denmark, Copenhagen, Denmark.
86. Knudsen GM, Olsen JE, Dons L. 2004. Characterization of DegU, a response regulator in *Listeria monocytogenes*, involved in regulation of motility and contributes to virulence. FEMS Microbiol Lett 240:171–179. https://doi.org/10.1016/j.femsle.2004.09.039.
87. Park S, Jung J, Choi S, Oh Y, Lee J, Chae H, Ryu S, Jung H, Park G, Choi S. 2012. Molecular characterization of *Listeria monocytogenes* based on the PFGE and RAPD in Korea. Adv Microbiol 2:26214. https://doi.org/10.4236/aim.2012.24079.